Multi-Phase Multi-Level AC Motor Drive Based on Four Three-Phase Two-Level Inverters

Gabriele Grandi, Angelo Tani, Padmanaban Sanjeevikumar, Darko Ostojic

Dept. of Electrical Engineering, University of Bologna
Viale Risorgimento, 2 - 40136 Bologna (IT)

***Abstract*—A novel multi-phase multi-level ac motor drive is analyzed in this paper. The proposed scheme is based on four conventional 2-level three-phase voltage source inverters (VSIs) supplying the open-end windings of a dual three-phase motor (asymmetric six-phase machine), quadrupling the power capability of a single VSI with given voltage and current ratings. The proposed control algorithm is able to generate multi-level voltage waveforms, equivalent to the ones of a 3-level inverter, and to share the total motor power among the four dc sources within each switching period. The proposed ac motor drive has been numerically implemented and a complete set of simulation results is given to prove the effectiveness of the whole scheme.**

***Index Terms*—Dual three-phase motors, multiple space vectors, space vector modulation, multilevel inverters, multiphase motor drives.**

I. Introduction

Multi-phase and multi-level inverter technologies have been widely recognized as a viable solution to overcome current and voltage limits of power switching converters in the area of high-power medium-voltage drive systems.

In particular, multi-phase motor drives have many advantages over the traditional three-phase motor drives, such as reducing the amplitude and increasing the frequency of torque pulsations, reducing the rotor harmonic current losses and lowering the dc link current harmonics. In addition, owing to their redundant structure, multi-phase motor drives improve the system reliability. As a consequence, the use of multi-phase inverters together with multi-phase ac machines has been recognized as a viable approach to obtain high power ratings with current limited devices [1]-[3].

On the other hand, multi-level converters are able to generate output voltage waveforms consisting in a large number of steps. In this way, high voltages can be synthesized using sources and switching devices with lower voltage values, with the additional benefit of a reduced harmonic distortion and lower dv/dt in the output voltages. For these reasons, the use of multi-level inverters has been recognized as a viable approach to obtain high power ratings with voltage limited devices [4]-[6].

It becomes evident that the combination of multi-phase and multi-level inverter technologies [7] could be an effective method to group the benefits of such technologies and to obtain high power ratings with both voltage- and current-limited devices.

Several conversion structures have been introduced in last decades for multi-phase and multi-level inverters. Among these structures, there are topologies based on a proper arrangement of conventional 2-level three-phase voltage source inverters (VSIs) to realize both multi-phase [8]-[12] and multi-level [13]-[17] inverters. The great advantages of such topologies are reliable power layout and effective protecting circuitry, reduced cost of both converter and motor due to conventional slot/winding configurations, and modularity of the whole conversion structure.

In order to exploit all these advantages, a novel structure based on a dual three-phase open-ends winding motor (asymmetric six-phase induction machine) has been considered in this paper. The power supply consists of four standard 2-level three-phase VSIs having insulated dc sources to prevent circulation of zero-sequence current components. A schematic diagram of the whole system is given in Fig. 1. Note that the structure is easy scalable to nine, twelve or higher number of phases multiple of three.

An original modulation strategy has been proposed to regulate each couple of 2-level VSIs such as a 3-level inverter, providing proper multi-level voltage waveforms for each three-phase stator winding. Furthermore, the proposed control algorithm allows total motor power to be shared among the four dc sources with three degrees of freedom, leading to a combination/extension of the power sharing principles given in [17] and [18]. Power sharing is a useful skill in battery supplied drives where the charge status of batteries should be balanced.

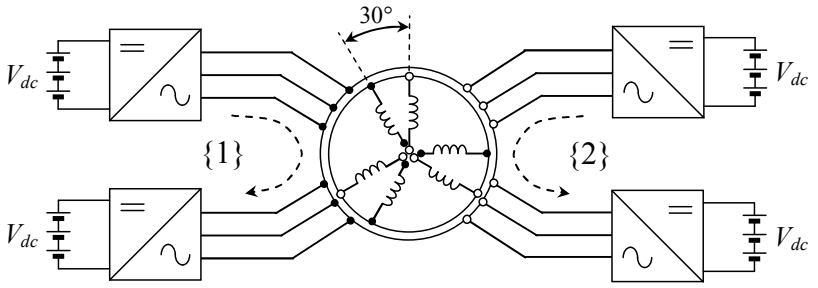

Fig. 1. Schematic diagram of the proposed multi-phase multi-level ac motor drive consisting in four voltage source inverters supplying a dual three-phase machine with open-end windings.

978-1-4244-7919-1/10/$25.00 ©2010 IEEE

II. Space Vector Transformations for Six-Phase Systems

Space vector transformations are introduced to represent the whole six-phase system consisting of the dual three-phase machine supplied by four insulated three-phase VSIs.

A. Multiple Space Vector Transformation

A possible space vector transformation for an asymmetric six-phase system leads to the following multiple space vectors [8], [12]

$$\begin{cases} \bar{x}_1 = \frac{1}{3}\left[x_1 + x_2\alpha + x_3\alpha^4 + x_4\alpha^5 + x_5\alpha^8 + x_6\alpha^9 \right] \\ \bar{x}_3 = \frac{1}{3}\left[(x_1 + x_3 + x_5) + j(x_2 + x_4 + x_6) \right] \\ \bar{x}_5 = \frac{1}{3}\left[x_1 + x_2\alpha^5 + x_3\alpha^8 + x_4\alpha + x_5\alpha^4 + x_6\alpha^9 \right] \end{cases}, \quad (1)$$

being $\alpha = exp\,(j\pi/6)$. The inverse transformation of (1) is given in [12]. The multiple space vectors $\bar{x}_1$, $\bar{x}_3$, and $\bar{x}_5$ lie in the planes here called d_1-q_1, d_3-q_3, and d_5-q_5, respectively.

B. Three-Phase Space Vector Decomposition

The six-phase system can be seen as the composition of two three-phase sub-systems {1} and {2} according to

$$\{1\}\begin{cases} x_1^{(1)} = x_1 \\ x_2^{(1)} = x_3 \\ x_3^{(1)} = x_5 \end{cases}, \quad \{2\}\begin{cases} x_1^{(2)} = x_2 \\ x_2^{(2)} = x_4 \\ x_3^{(2)} = x_6 \end{cases}. \quad (2)$$

The space vectors $\bar{x}^{(1)}$, $\bar{x}^{(2)}$ and the zero-sequence components $x_0^{(1)}$, $x_0^{(2)}$ can be defined for each three-phase sub-system {1}, {2}, leading to

$$\begin{cases} \bar{x}^{(1)} = \frac{2}{3}\left[x_1^{(1)} + x_2^{(1)}\alpha^4 + x_3^{(1)}\alpha^8 \right] \\ x_0^{(1)} = \frac{1}{3}\left[x_1^{(1)} + x_2^{(1)} + x_3^{(1)} \right] \end{cases} \cdot \quad (3)$$
$$\begin{cases} \bar{x}^{(2)} = \frac{2}{3}\left[x_1^{(2)} + x_2^{(2)}\alpha^4 + x_3^{(2)}\alpha^8 \right] \\ x_0^{(2)} = \frac{1}{3}\left[x_1^{(2)} + x_2^{(2)} + x_3^{(2)} \right] \end{cases}$$

The relationships between multiple space vectors and three-phase space vectors are obtained by introducing (2) and (3) in (1), leading to

$$\begin{cases} \bar{x}_1 = \frac{1}{2}\left[\bar{x}^{(1)} + \alpha\,\bar{x}^{(2)} \right] \\ \bar{x}_5^* = \frac{1}{2}\left[\bar{x}^{(1)} - \alpha\,\bar{x}^{(2)} \right] \end{cases}, \quad \bar{x}_3 = x_0^{(1)} + j x_0^{(2)}, \quad (4)$$

$$\begin{cases} \bar{x}^{(1)} = \bar{x}_1 + \bar{x}_5^* \\ x_0^{(1)} = \bar{x}_3 \cdot 1 \end{cases}, \quad \begin{cases} \bar{x}^{(2)} = \alpha^{-1}\left(\bar{x}_1 - \bar{x}_5^* \right) \\ x_0^{(2)} = \bar{x}_3 \cdot j \end{cases}, \quad (5)$$

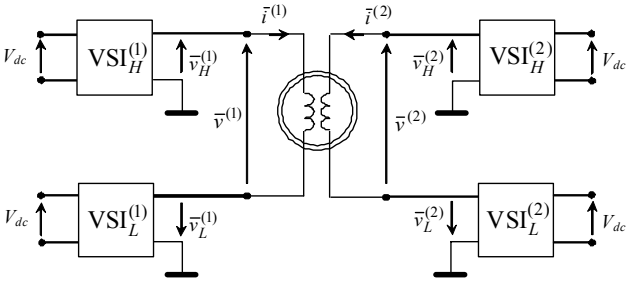

Fig. 2. Equivalent circuit of the whole ac motor drive in terms of three-phase space vectors.

where the symbols " * " and " · "denote complex conjugate and scalar (dot) product, respectively.
The representation of the proposed multi-phase multilevel ac motor drive shown in Fig. 1 in terms of three-phase space vectors leads to the schematic equivalent circuit of Fig. 2.

III. Dual Three-Phase Induction Motor Drive

For the ac motor drive, an induction machine has been considered in this paper.

A. Machine Model by Multiple Space Vectors

The behavior of the dual three-phase induction machine having sinusoidal distributed stator windings can be described in terms of multiple space vectors by the following equations, written in a stationary reference frame:

$$\bar{v}_{S1} = R_S\,\bar{i}_{S1} + \frac{d\bar{\varphi}_{S1}}{dt}, \quad \bar{\varphi}_{S1} = L_{S1}\,\bar{i}_{S1} + M_1\,\bar{i}_{R1}, \quad (6)$$

$$0 = R_R\,\bar{i}_{R1} - j\,p\,\omega_m\,\bar{\varphi}_{R1} + \frac{d\bar{\varphi}_{R1}}{dt}, \quad \bar{\varphi}_{R1} = M_1\,\bar{i}_{S1} + L_{R1}\,\bar{i}_{R1}, \quad (7)$$

$$\bar{v}_{S5} = R_S\,\bar{i}_{S5} + \frac{d\bar{\varphi}_{S5}}{dt}, \quad \bar{\varphi}_{S5} = L_{S\ell}\,\bar{i}_{S5}, \quad (8)$$

$$T = 3\,p\,M_1\,\bar{i}_{S1} \cdot j\,\bar{i}_{R1}, \quad (9)$$

where p is the pole pairs number, ω_m is the rotor angular speed, and the subscripts S and R denote stator and rotor quantities, respectively. It should be noted that $\bar{i}_{S1}$ and $\bar{i}_{R1}$ are responsible for the sinusoidal spatial distribution of the magnetic field in the air gap, whereas $\bar{i}_{S5}$ does not contribute to the air gap field.

B. Field Oriented Control

In dual three-phase induction motor drives, the reference values of the d_1-q_1 components of the stator currents in a synchronous reference frame, $i_{1d,ref}$ and $i_{1q,ref}$, are determined on the basis of flux and torque commands, respectively [11]. The d-axis of synchronous reference frame is aligned with the rotor flux, displaced by angle ϑ with respect to the d-axis stationary reference frame.

Then, the reference values of the stator voltage space vectors in a stationary reference frame, $\bar{v}_{S1,ref}$ and $\bar{v}_{S5,ref}$ can be determined by the typical block diagram represented in Fig. 3. Note that the condition $\bar{v}_{S5,ref} = 0$ leads to balanced power sharing between the two three-phase stator windings.

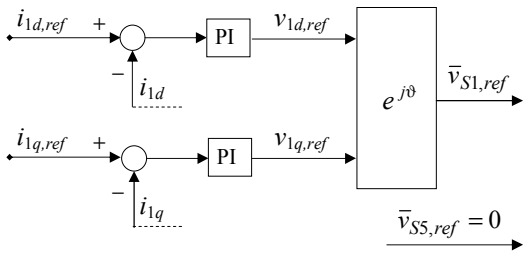

Fig. 3. Block diagram of a typical current controller in the synchronous reference frame for dual three-phase induction motor drives.

IV. Power Sharing Management

In the proposed system, the power sharing among the four dc sources is characterized by three degrees of freedom. The first one concerns the power sharing between the two three-phase windings {1} and {2}, whereas second and third ones are related to the power sharing between the two inverters H and L which supply each three-phase winding.

A. Power Sharing Between Two Windings {1} and {2}

According to (4), the stator current space vector $\bar{i}_{S1}$, which is determined on the basis of torque and flux demands, can be expressed as

$$\bar{i}_{S1} = \frac{1}{2}\left(\bar{i}^{(1)} + \alpha \bar{i}^{(2)}\right). \tag{10}$$

In order to minimize the currents in the two three-phase windings, the space vectors $\bar{i}^{(1)}$ and $\alpha\bar{i}^{(2)}$ have to be in phase, therefore the following assumption can be made:

$$\begin{cases} \frac{1}{2}\bar{i}^{(1)} = k_i\, \bar{i}_{S1} \\ \frac{1}{2}\alpha \bar{i}^{(2)} = (1-k_i)\,\bar{i}_{S1} \end{cases}, \tag{11}$$

where k_i represents a currents ratio between the windings.

The expressions of $\bar{i}^{(1)}$ and $\bar{i}^{(2)}$ can be readily obtained from (11), leading to

$$\begin{cases} \bar{i}^{(1)} = 2k_i\, \bar{i}_{S1} \\ \bar{i}^{(2)} = 2(1-k_i)\,\alpha^{-1}\, \bar{i}_{S1} \end{cases}. \tag{12}$$

Once the three-phase current space vectors are known, the stator current space vector $\bar{i}^{*}_{S5}$ can be determined by introducing (12) in (4):

$$\bar{i}^{*}_{S5} = \frac{1}{2}\left(\bar{i}^{(1)} - \alpha \bar{i}^{(2)}\right) = (2k_i - 1)\bar{i}_{S1}. \tag{13}$$

Rewriting (13) in the synchronous reference frame, the relationship in terms of *d*-*q* components becomes

$$\begin{cases} i_{5d} = (2k_i - 1) i_{1d} \\ i_{5q} = -(2k_i - 1) i_{1q} \end{cases}. \tag{14}$$

As emphasized in the block diagram shown in Fig. (4) and according to (14), the d_5-q_5 components of the reference current can be directly determined on the basis of the corresponding d_1-q_1 components and the current ratio.

The related reference stator voltages in the synchronous reference frame are then obtained by means of conventional PI regulators, acting on the error signals. Finally, the reference stator voltages in the stationary reference frame, $\bar{v}_{S1,ref}$ and $\bar{v}^{*}_{S5,ref}$, which represent the inputs of the modulation process, are determined through an opportune angular rotation.

It can be shown that the current ratio k_i introduced in (11) corresponds, with a good approximation, to a sharing coefficient of the motor power P between the two three-phase windings. In particular, the total electric power supplied to the motor can be written as [3]

$$P = P^{(1)} + P^{(2)} = 3\bar{v}_{S1} \cdot \bar{i}_{S1} + 3\bar{v}_{S5} \cdot \bar{i}_{S5}, \tag{15}$$

$$\begin{cases} P^{(1)} = \frac{3}{2}\bar{v}^{(1)} \cdot \bar{i}^{(1)} \\ P^{(2)} = \frac{3}{2}\bar{v}^{(2)} \cdot \bar{i}^{(2)} \end{cases}. \tag{16}$$

On the basis of (5), the space vectors of the three-phase stator currents and voltages can be calculated as follows

$$\begin{cases} \bar{i}^{(1)} = \bar{i}_{S1} + \bar{i}^{*}_{S5} \\ \bar{i}^{(2)} = \alpha^{-1}\,(\bar{i}_{S1} - \bar{i}^{*}_{S5}) \end{cases}, \tag{17}$$

$$\begin{cases} \bar{v}^{(1)} = \bar{v}_{S1} + \bar{v}^{*}_{S5} \\ \bar{v}^{(2)} = \alpha^{-1}\,(\bar{v}_{S1} - \bar{v}^{*}_{S5}) \end{cases}. \tag{18}$$

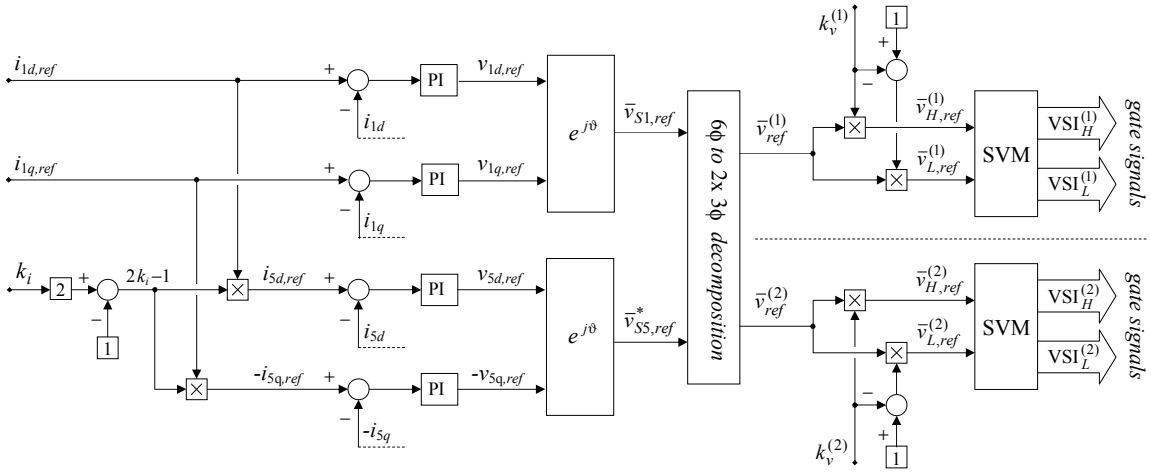

Fig. 4. Block diagram of the proposed regulation scheme with power sharing capabilities for dual three-phase induction motor drives.

Substituting (17) and (18) in (16), and taking (13) into account yields

$$\begin{cases} P^{(1)} = 3k_i\,\bar{v}_{S1}\cdot\bar{i}_{S1} + 3k_i\,\bar{v}^{*}_{S5}\cdot\bar{i}_{S1} \\ P^{(2)} = 3(1-k_i)\,\bar{v}_{S1}\cdot\bar{i}_{S1} - 3(1-k_i)\,\bar{v}^{*}_{S5}\cdot\bar{i}_{S1} \end{cases}. \tag{19}$$

As can be recognized analyzing the dual three-phase motor model, in particular (6) and (8), the voltage space vector $\bar{v}^{*}_{S5}$ can be considered negligible with respect to $\bar{v}_{S1}$. Then, comparing (15) and (19) leads to

$$\begin{cases} P^{(1)} \cong k_i\,P \\ P^{(2)} \cong (1-k_i)\,P \end{cases}. \tag{20}$$

Eqs. (20) confirm that the current ratio k_i defined by (11) can be practically considered also a power sharing coefficient between the three-phase windings {1} and {2}.

B. Power Sharing Between Two Inverters H and L

The reference output voltage $\bar{v}^{(1)}_{ref}$ supplying the first three-phase stator winding can be determined by the six- to three-phase decomposition (18), on the basis of multiple space vector references $\bar{v}_{S1,ref}$ and $\bar{v}^{*}_{S5,ref}$. In particular, $\bar{v}^{(1)}_{ref}$ can be synthesized as the sum of the voltages $\bar{v}^{(1)}_{H,ref}$ and $\bar{v}^{(1)}_{L,ref}$ generated by $\mathrm{VSI}^{(1)}_{H}$ and $\mathrm{VSI}^{(1)}_{L}$, respectively, leading to

$$\bar{v}^{(1)}_{ref} = \bar{v}^{(1)}_{H,ref} + \bar{v}^{(1)}_{L,ref}. \tag{21}$$

Introducing the voltage ratio $k^{(1)}_{v}$ and imposing the inverter voltage vectors $\bar{v}^{(1)}_{H,ref}$ and $\bar{v}^{(1)}_{L,ref}$ to be in phase with the output voltage vector $\bar{v}^{(1)}_{ref}$, yields

$$\begin{cases} \bar{v}^{(1)}_{H,ref} = k^{(1)}_{v}\,\bar{v}^{(1)}_{ref} \\ \bar{v}^{(1)}_{L,ref} = \left(1-k^{(1)}_{v}\right)\bar{v}^{(1)}_{ref} \end{cases}. \tag{22}$$

The condition expressed by (22) allows maximum dc voltage utilization. Being the output ac current of the two inverters the same, the coefficient $k^{(1)}_{v}$ also defines the power sharing between the two inverters. In terms of averaged values within the switching period, the power to the first three-phase stator winding can be expressed as

$$P^{(1)} = \frac{3}{2}\bar{v}^{(1)}_{ref}\cdot\bar{i}^{(1)} = P^{(1)}_{H} + P^{(1)}_{L}, \tag{23}$$

where $P^{(1)}_{H}$ and $P^{(1)}_{L}$ are the individual powers from the two inverters. By combining (22) with (23) leads to

$$\begin{cases} P^{(1)}_{H} = \frac{3}{2}\bar{v}^{(1)}_{H,ref}\cdot\bar{i}^{(1)} = k^{(1)}_{v}\,P^{(1)} \\ P^{(1)}_{L} = \frac{3}{2}\bar{v}^{(1)}_{L,ref}\cdot\bar{i}^{(1)} = \left(1-k^{(1)}_{v}\right)P^{(1)} \end{cases}. \tag{24}$$

The coefficient $k^{(1)}_{v}$ has a limited variation range depending on the value of the reference output voltage $\bar{v}^{(1)}_{ref}$, as already investigated in [17].

Furthermore, it has to be verified that both references are within the range of achievable output voltages of each inverter, which depend on their dc voltages. In the case of a single inverter topology, if the voltage demand exceeds the voltage limit, the output voltage is simply saturated. With the dual inverter configuration, total voltage reference must be satisfied, so in case of voltage saturation of one inverter, the second has to provide for the missing part. A possible solution to overcome the problems of voltage saturation in the dual inverter configuration has been proposed in [17].

An identical approach can be applied to synthesize the voltage $\bar{v}^{(2)}_{ref}$ supplying the second three-phase stator winding by inverters $\mathrm{VSI}^{(2)}_{H}$ and $\mathrm{VSI}^{(2)}_{L}$, leading to

$$\bar{v}^{(2)}_{ref} = \bar{v}^{(2)}_{H,ref} + \bar{v}^{(2)}_{L,ref}. \tag{25}$$

As in the preceding case, introducing the voltage ratio $k^{(2)}_{v}$ leads to

$$\begin{cases} \bar{v}^{(2)}_{H,ref} = k^{(2)}_{v}\,\bar{v}^{(2)}_{ref} \\ \bar{v}^{(2)}_{L,ref} = \left(1-k^{(2)}_{v}\right)\bar{v}^{(2)}_{ref} \end{cases}. \tag{26}$$

The powers to the second three-phase stator winding now become

$$P^{(2)} = \frac{3}{2}\bar{v}^{(2)}_{ref}\cdot\bar{i}^{(2)} = P^{(2)}_{H} + P^{(2)}_{L}, \tag{27}$$

$$\begin{cases} P^{(2)}_{H} = \frac{3}{2}\bar{v}^{(2)}_{H,ref}\cdot\bar{i}^{(2)} = k^{(2)}_{v}\,P^{(2)} \\ P^{(2)}_{L} = \frac{3}{2}\bar{v}^{(2)}_{L,ref}\cdot\bar{i}^{(2)} = \left(1-k^{(2)}_{v}\right)P^{(2)} \end{cases}. \tag{28}$$

Same considerations given for $k^{(1)}_{v}$ now apply to $k^{(2)}_{v}$.

V. Multilevel SVM Algorithm

Once the reference voltage vectors $\bar{v}^{(1)}_{ref}$ and $\bar{v}^{(2)}_{ref}$ for the two couples of inverters are determined by (22) and (26), a proper multilevel SVM algorithm must be applied to satisfy the power sharing imposed by $k^{(1)}_{v}$ and $k^{(2)}_{v}$, according to the block diagram of Fig. 4.

In particular, the SVM algorithm considered in this paper is based on the space vector diagram given in Fig. 5. Due to the symmetry of the outer hexagon, the analysis can be restricted to one of its six sectors (i.e., OAB in Fig. 5), similarly to the case of conventional three-phase SVM algorithm. Furthermore, the main triangle OAB is divided in four identical equilateral triangles.

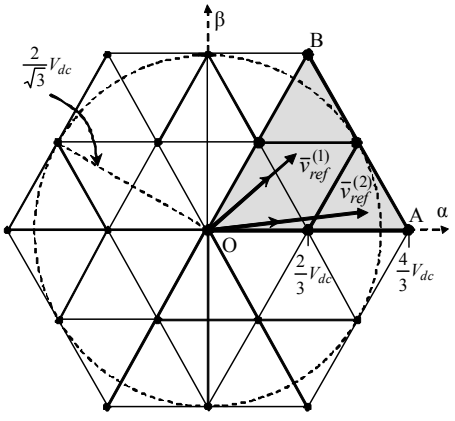

Fig. 5. Plot of voltage space vectors generated by inverters H and L for both the stator windings {1} and {2}.

The reference voltage $\bar{v}_{ref}^{(1)}$ lays in one of these triangles, leading to four relevant cases. By the basic SVM principle, the components $\bar{v}_{H,ref}^{(1)}$ and $\bar{v}_{L,ref}^{(1)}$ can be generated by selecting adjacent vectors. The switch configurations corresponding to these vectors cannot be applied in an arbitrary sequence if proper multilevel voltage waveforms are desired, i.e., the reference voltage $\bar{v}_{ref}^{(1)}$ should be generated by using the nearest three vectors approach (NTV) [19]. In order to do this, the method introduced in [17] has been implemented. The same considerations apply to the reference voltage $\bar{v}_{ref}^{(2)}$.

VI. Results

In order to verify the effectiveness of the proposed control strategy, the behavior of the whole system has been numerically tested by means of the PLECS simulation package in the MATLAB environment.

For the induction motor, the model presented in Section III has been implemented using the parameters given in Table I. The value of the four dc bus voltages (V_{dc}) is set to 155 V and a switching frequency of 5 kHz is selected.

In the first simulation test (Figs. 6-10), the behavior of the system is analyzed in balanced conditions ($k_i = 0.5$, $k_v^{(1)} = k_v^{(2)} = 0.5$), i.e. the electrical power is equally shared among the four VSIs. A torque step is demanded to emphasize dynamics, as depicted in Fig. 6. The corresponding six stator currents are shown in Fig. 7. It should be noted that the current waveforms are practically sinusoidal, with the same amplitude, and correct phase angle displacements.

TABLE I
MOTOR PARAMETERS

P_{rated}	= 8 kW	R_S	= 0.51 Ω
$I_{S,\,rated}$	= 16 A_{rms}	R_R	= 0.42 Ω
$V_{S,rated}$	= 125 V_{rms}	L_{S1}	= 58.2 mH
$\omega_{S,rated}$	= 2π50 rad/s	L_{R1}	= 58.2 mH
p	= 2 (pairs)	M_1	= 56 mH

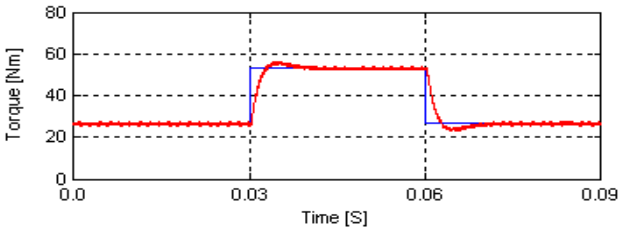

Fig. 6. Step change between 50% and 100% of the rated torque.

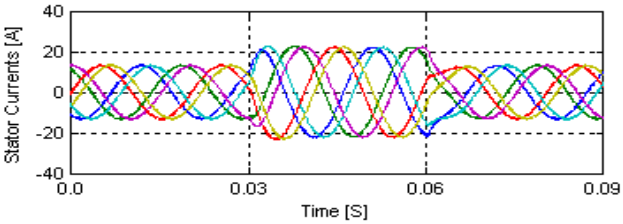

Fig. 7. Stator currents waveforms during the torque step.

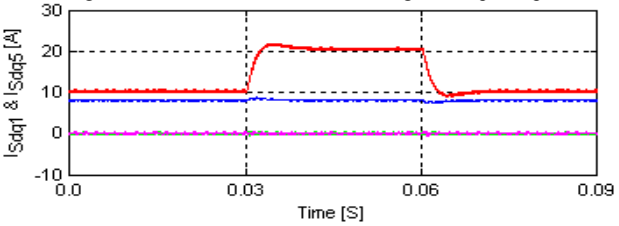

Fig. 8. *d-q* current components (from top to bottom): i_{1q}, i_{1d}, i_{5q}, i_{5d}.

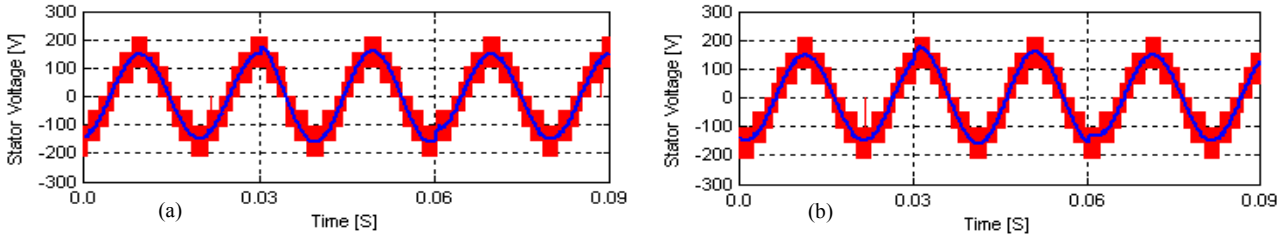

Fig. 9. Stator phase voltage waveforms during the torque step: (a) voltage $v_1^{(1)}$, (b) voltage $v_1^{(2)}$.

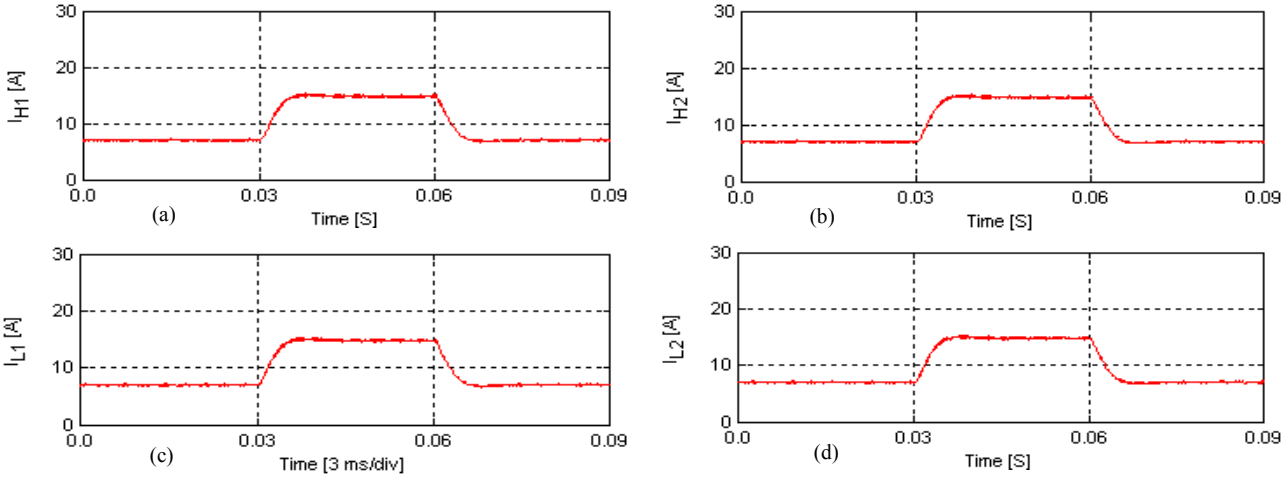

Fig. 10. Inverter dc currents during the torque step (low-pass filtered, τ = 2 ms).

In Fig. 8 the d_1-q_1 and d_5-q_5 stator current components in the synchronous reference frame are depicted. Note that i_{5q} and i_{5d} are null being the current ratio k_i set to 0.5 (balanced), according to (14), whereas i_{1q} and i_{1d} follow torque and rotor flux commands.

Fig. 9 shows the nine-level waveforms of phase voltages $v_1^{(1)}$ (stator voltage of phase 1 of the first three-phase winding) and $v_1^{(2)}$ (stator voltage of phase 1 of the second three-phase winding). The averaged voltage value is also depicted in the same diagrams.

Fig. 10 shows dc currents of the four VSIs during the torque step. The instantaneous values have been averaged by a low-pass filter (τ = 2 ms). The diagrams confirm a balanced dc current sharing among all inverters, i.e., balanced power sharing, as stated by (20), (24) and (28).

In the second simulation test (Figs. 11-16), torque and flux commands are maintained constant. The current ratio k_i has been changed among the values 1/2, 1/3 and 2/3, as shown in Fig. 11, to emphasize the power sharing capability between the two motor windings. The voltage ratio coefficients $k_v^{(1)}$ and $k_v^{(2)}$ are fixed to 0.5.

The torque is unaffected by this transient, as shown in Fig. 12, whereas the stator current amplitudes of windings {1} and {2} change according to (12), as depicted in Fig. 13. The d_1-q_1 and d_5-q_5 stator current components in the synchronous reference are shown in Fig. 14. As expected, i_{1d} and i_{1q} are constant, whereas i_{5d} and i_{5q} vary according to (14).

The waveforms of phase voltages $v_1^{(1)}$ and $v_1^{(2)}$, together with the corresponding averaged values, are depicted in Figs. 15a and 15b, respectively.

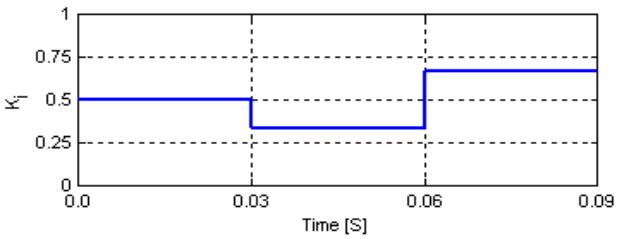

Fig. 11. Variation of the current ratio coefficient k_i.

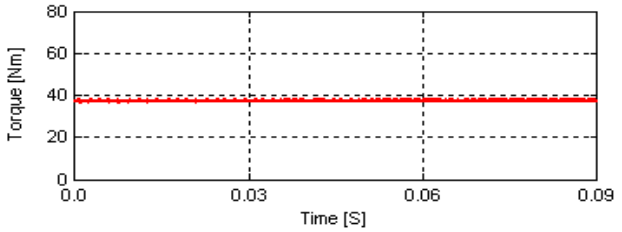

Fig. 12. Torque behavior during the variation of k_i.

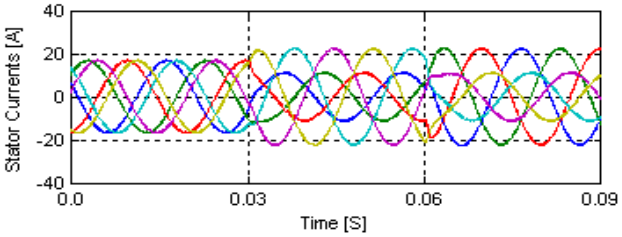

Fig. 13. Stator current waveforms during the variation of k_i.

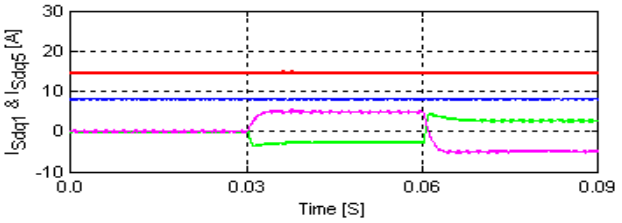

Fig. 14. d-q current components (from top to bottom): i_{1q}, i_{1d}, i_{5q}, i_{5d}.

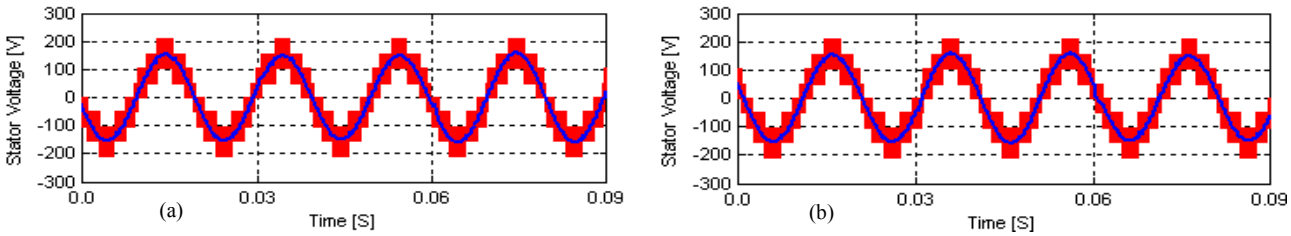

Fig. 15. Stator phase voltage waveforms during the variation of k_i: (a) voltage $v_1^{(1)}$, (b) voltage $v_1^{(2)}$.

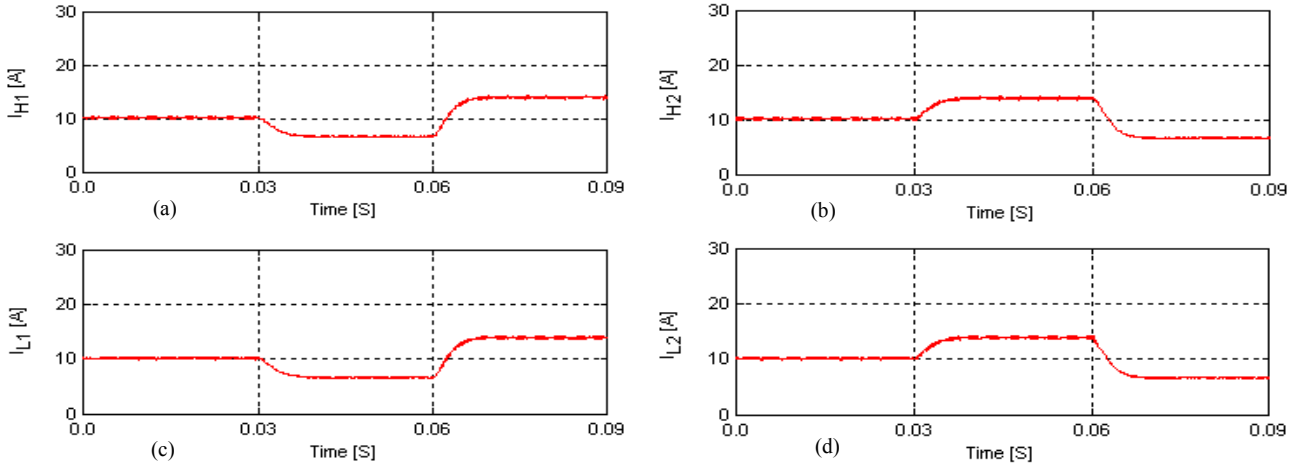

Fig. 16. Inverter dc currents during the variation of k_i (low-pass filtered, τ = 2 ms).

Figs. 16 emphasize the low-pass filtered value of the four dc currents. Owing to $k_v^{(1)} = k_v^{(2)} = 0.5$, the dc currents of inverters {1} are equal (see Figs. 16a and 16c) and the same holds for the dc currents of inverters {2} (see Figs. 16b and 16d). On the contrary, the dc currents of inverters {1} and {2} become different as k_i changes from 0.5, due to the power sharing variation between the two windings, as stated by (20).

In last simulation test (Figs. 17-22), the power sharing capability between the two inverters H and L of each three-phase stator winding has been emphasized while both torque and flux commands are kept constant. The voltage ratios $k_v^{(1)}$ and $k_v^{(2)}$ have been changed between the values 1/2, 1/3 and 1/2, 2/3, respectively, at different time instants, as shown in Fig. 17. In this case, the current ratio coefficient k_i is fixed to 0.5. As expected, these changes do not affect the torque and the six stator currents, as proved by Figs. 18 and 19, respectively.

The d_1-q_1 and d_5-q_5 stator current components in the synchronous reference are shown in Fig. 20. Note that i_{5q} and i_{5d} are null being the current ratio k_i set to 0.5, whereas the constant values of i_{1q} and i_{1d} are determined by torque and rotor flux references, respectively.

Fig. 21a and 21b show the waveforms of phase voltages $v_1^{(1)}$ and $v_1^{(2)}$, respectively, together with their averaged values.

Figs. 22 emphasize the low-pass filtered values of the four dc currents. Owing to $k_i = 0.5$, the sum of dc currents of inverters {1} (proportional to $P^{(1)}$) is constant and equal to the sum of dc currents of inverters {2} (proportional to $P^{(2)}$), whereas each dc current and its corresponding dc power change according to (24) and (28).

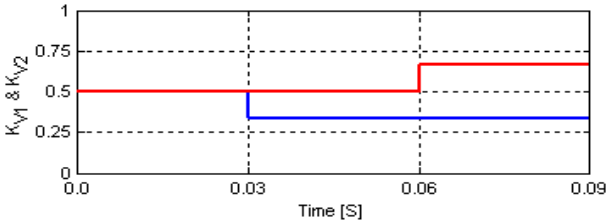

Fig. 17. Step variation of voltage ratios $k_v^{(1)}$ (0.03 s) and $k_v^{(2)}$ (0.06 s).

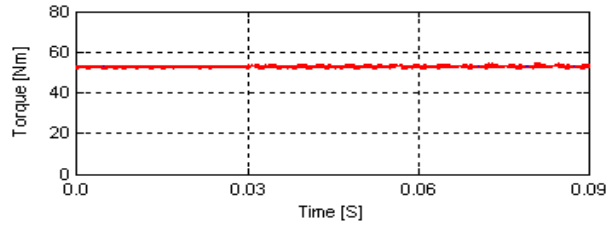

Fig. 18. Torque behavior during the variation of $k_v^{(1)}$ and $k_v^{(2)}$.

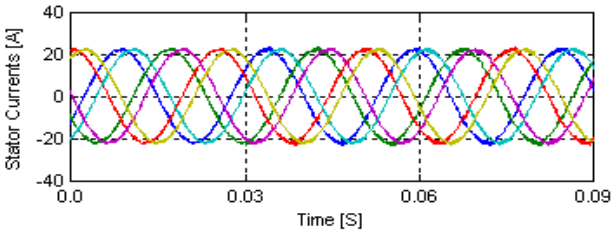

Fig. 19. Stator current waveforms during the variation of $k_v^{(1)}$ and $k_v^{(2)}$.

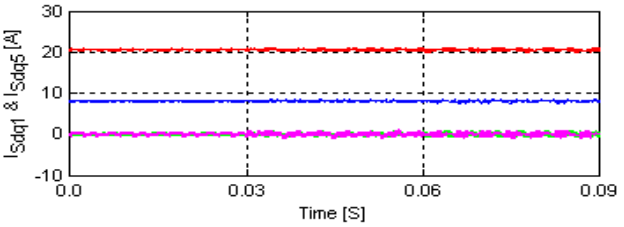

Fig. 20. *d-q* current components (from top to bottom): i_{1q}, i_{1d}, i_{5q}, i_{5d}.

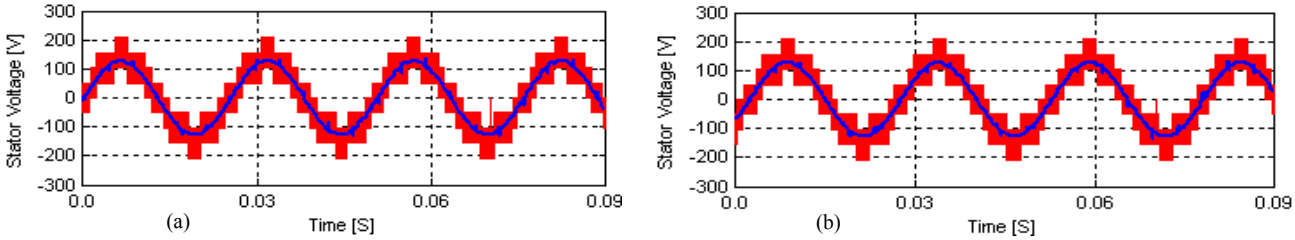

Fig. 21. Stator phase voltage waveforms during the variation of $k_v^{(1)}$ and $k_v^{(2)}$: (a) voltage $v_1^{(1)}$, (b) voltage $v_1^{(2)}$.

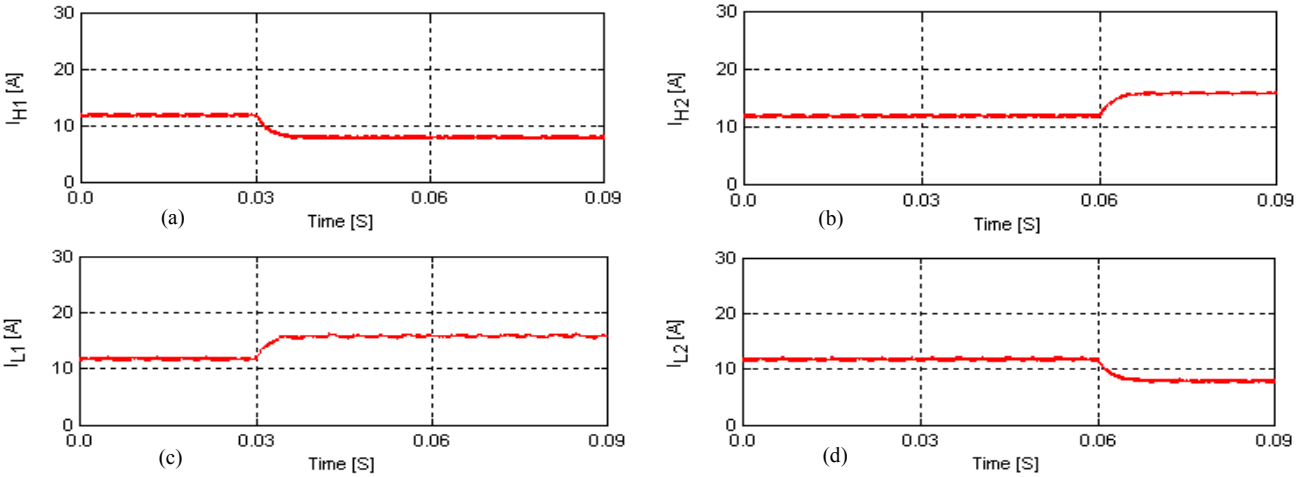

Fig. 22. Inverter dc currents during the variation of $k_v^{(1)}$ and $k_v^{(2)}$ (low-pass filtered, $\tau = 2$ ms).

VII. Conclusion

A new multi-phase multi-level ac motor drive based on a dual three-phase open-end windings induction machine has been presented and analyzed in this paper. The power supply consists of four conventional 2-level three-phase voltage source inverters with insulated dc sources.

An appropriate control strategy which allows the total motor power to be shared among the four dc sources with three degrees of freedom has been proposed.

In order to regulate the couple of 2-level VSIs supplying each three-phase winding such as a 3-level inverter, a specific SVM technique has been adopted, allowing the power sharing between the two dc sources. This regulation leads to two degrees of freedom in the total power sharing, one for each three-phase winding.

A suitable technique has been proposed in order to regulate the power sharing between the two three-phase windings, leading to an additional degree of freedom in the total power sharing.

Numerical tests provided in the paper prove the effectiveness of the proposed multi-phase multi-level ac motor drive in different operating conditions. The hardware prototype of the whole ac motor drive system is actually under development.

References

[1] E. Levi, R. Bojoi, F. Profumo, H.A. Toliyat, and S. Williamson, "Multiphase induction motor drives – a technology status review," *IET Electr. Power Appl.*, vol. 1, no. 4, pp. 489-516, July 2007.

[2] E. Levi, "Multiphase electric machines for variable-speed applications," *IEEE Trans. Ind. Electron.*, vol. 55, no. 5, pp. 1893–1909, May 2008.

[3] G. Grandi, G. Serra, and A. Tani, "General analysis of multiphase systems based on space vector approach," *in Proc. Inter. Power Electronics and Motion Control Conf.*, EPE-PEMC, Portoroz, Slovenia, 30 Aug.–1 Sep. 2006, pp. 834-840.

[4] J. Rodríguez, J.S. Lai, F. Zheng Peng, "Multilevel inverters: A survey of topologies, controls, and applications," *IEEE Trans. on Industry Electronics*, Vol. 49, no. 4, pp. 724-738, Aug. 2002.

[5] J. Rodriguez, S. Bernet, Bin Wu, J.O. Pontt, S. Kouro, "Multilevel voltage-source-converter topologies for industrial medium-voltage drives," *IEEE Trans. Ind. Electron.,* vol. 54, no. 6, Dec 2007, pp. 2930-2945.

[6] L. G. Franquelo, J. Rodriguez, J. I. Leon, S. Kouro, R. Portillo and M. M. Prats, "The age of multilevel converters arrives," *IEEE Ind. Electron. Magazine*, vol. 2, no. 2, pp. 28–39, June 2008.

[7] O. López, J. Alvarez, J. Doval-Gandoy, and F. D. Freijedo, "Multilevel multiphase space vector PWM algorithm," *IEEE Trans. Ind. Electron.*, vol. 55, no. 5, pp. 1933-1942, May 2008.

[8] Y. Zhao, T.A. Lipo, "Space vector PWM control of dual three-phase induction machine using vector space decomposition," *IEEE Trans. on Ind. Applicat.*, vol. 31, no. 5, pp. 1100-1109, September/October 1995.

[9] K.K. Mohapatra, R.S. Kanchan, M.R. Baiju, P.N. Tekwani, K. Gopakumar, "Independent Field-Oriented control of two split-phase induction motors from a single six-phase inverter," *IEEE Trans. on Ind. Electron.*, vol. 52, no. 5, pp. 1372-1382, October 2005.

[10] D. Hadiouche, L. Baghli, A. Rezzoug, "Space vector PWM techniques for dual three-phase AC machine: analysis, performance evaluation and DSP implementation," *IEEE Trans. on Ind. Applicat.,* vol. 42, no. 4, pp. 1112-1122, July/August 2006.

[11] R. Bojoi, F. Farina, F. Profumo, A. Tenconi, "Dual-three phase induction machine drives control – a Survey," *IEEJ Transaction on IA,* Vol. 126, no. 4, pp. 420-429, 2006.

[12] G. Grandi, A. Tani, G. Serra: "Space vector modulation of six-phase VSI based on three-phase decomposition", *19th Symposium on Power Electronics, Electrical Drives etc., SPEEDAM*, Taormina (IT), June 11-13, 2008, pp. 674-679.

[13] Y. Kawabata, M. Nasu, T. Nomoto, E.C. Ejiogu, T.Kawabata, "High-efficiency and low acoustic noise drive system using open-winding AC motor and two space-vector-modulated inverters," *IEEE Trans. on Ind. Electronics*, Vol. 49, no. 4, August 2002, pp. 783-789.

[14] J. Kim, J. Jung, and K. Nam, "Dual-inverter control strategy for high-speed operation of EV induction motors," *IEEE Trans. Ind. Electron*., vol. 51, no. 2, pp. 312- 320, Apr. 2004.

[15] M. B. Baiju, K.K. Mohapatra, R.S. Kanchan and K. Gopakumar, "A dual two-level inverter scheme with common mode voltage elimination for an induction motor drive", *IEEE Trans. Power Electron.* vol. 19, no. 3, pp. 794-805, May 2004.

[16] R. Kanchan, P. Tekwani, and K. Gopakumar, "Three-level inverter scheme with common mode voltage elimination and dc link capacitor voltage balancing for an open-end winding induction motor drive," *IEEE Trans. Power Electron.*, vol. 21, no. 6, pp. 1676-1683, Nov. 2006.

[17] C. Rossi, D. Casadei, G. Grandi, A. Lega, "Multilevel operation and input power balancing for a dual two-level inverter with insulated DC sources", IEEE *Trans. on Industry Applications*, vol. 44, no. 6, Nov/Dec 2008. pp. 1815-1824.

[18] R. Bojoi, A. Tenconi, F. Farina, F. Profumo, "Dual-source fed multi-phase induction motor drive for fuel cell vehicles: Topology and control," *Proc. of 36th Power Electronics Specialists Conference*, PESC 2005, June 2005, Recife, Brasil, pp. 2676-2683.

[19] D.G. Holmes, T.A. Lipo, *Pulse width modulation for power converters: Principles and practice*, IEEE Press/John Wiley, 2003, pp. 467–469.